avirulent strains of *Pseudomonas solanacearum* were agglutinated by potato lectin whereas no agglutination occurred with the virulent strains, even though both strains had a lipopolysaccharide capable of reacting with the potato lectin. However, the virulent strain carried an extracellular polysaccharide that apparently prevented the binding of the lectin to bacterial surfaces (*8*). If the extracellular polysaccharide was removed from the virulent bacteria, they also agglutinated with the potato lectin (*8*). The agglutination of *P. phaseolicola* and *P. tomato* by bean lectins may be prevented by a similar mechanism. If lectins are involved in the initial attachment of bacteria to plant cell walls, the lectins should be present at the surface of the cell wall. To our knowledge, such localization has not been demonstrated.

The encapsulation material has been described in tobacco as a cuticular layer (*3*) or a pellicle surrounding granular material (*4*). In beans there is less evidence of a discrete pellicle and the encapsulation material appears fibrillar rather than granular. Another striking difference between the tobacco and bean systems is in the area of the processes leading to the hypersensitive response. Attachment and encapsulation of avirulent strains of *P. solanacearum* by tobacco cells appear to be essential steps leading to the hypersensitive response (*4*). Attachment and encapsulation of *Pseudomonas pisi* (pathogenic on pea but not tobacco) also takes place in tobacco before the observation of hypersensitivity (*3*). However, *P. tomato* induces the hypersensitive response in the nonhost bean without either attachment or encapsulation of the bacterial cells, and consequently these steps do not appear to be prerequisite for hypersensitivity in 'Red Kidney' beans.

The active and rapid response of the plant cells to saprophytic bacteria make this an interesting system for studying the molecular mechanisms of recognition at the cell surface.

VENANCIO O. SING
MILTON N. SCHROTH
Department of Plant Pathology, University of California, Berkeley 94720

References and Notes

1. C. E. Yarwood, *Phytopathology* **63**, 1324 (1973).
2. D. C. Hildebrand and M. N. Schroth, *ibid.* **58**, 354 (1968).
3. R. N. Goodman, P-Y. Huang, J. A. White, *ibid.* **66**, 754 (1976).
4. L. Sequeira, G. Gaard, G. A. De Zoetten, *Physiol. Plant Pathol.* **10**, 43 (1977).
5. A. R. Spurr, *J. Ultrastruct. Res.* **26**, 31 (1969).
6. D. C. Hildebrand, *Phytopathology* **63**, 301 (1973); N. T. Keen and B. W. Kennedy, *Physiol. Plant Pathol.* **4**, 173 (1974); S. S. Patil and S. S. Gnanamanickam, *Nature (London)* **259**, 486 (1976).
7. J. E. DeVay and H. E. Adler, *Annu. Rev. Microbiol.* **30**, 147 (1976); J. Hamblin and S. P. Kent, *Nature (London)* **245**, 28 (1973); B. B. Bohlool and E. L. Schmidt, *Science* **185**, 269 (1974); *J. Bacteriol.* **125**, 1188 (1976); F. B. Dazzo and D. H. Hubbell, *Appl. Microbiol.* **30**, 1017 (1975); F. B. Dazzo, C. A. Napoli, D. H. Hubbell, *Appl. Environ. Microbiol.* **32**, 166 (1976).
8. L. Sequeira and T. L. Graham, in preparation.
9. The authors are greatly indebted to D. C. Hildebrand for many useful discussions and valuable help in the preparation of this manuscript and to C. E. Ballou, O. C. Huisman, and A. R. Weinhold for their review and critique of the manuscript.

10 March 1977; revised 3 May 1977

Phase Control of Neural Pacemakers

Abstract. *An electrical stimulus resets the phase of a spontaneously rhythmic neuron. The "new phase" versus "old phase" curve shows either of two distinct topological characters, depending on the stimulus magnitude. These features, and a phase singularity implicit in them, are common to many stable oscillations deriving from continuous feedback between two or more biophysical quantities.*

A quarter-century ago, Hodgkin and Huxley (*1*) simultaneously established a paradigm for inquiry into the ionic basis of electrical activity in nerve membrane and gave a quantitative description of action potentials in squid axon, using a system of ordinary differential equations. Their dynamical model (the set of equations) has undergone diverse revisions to improve its precision (for example, by adding a fifth, slower-moving quantity), and to adapt it to use with other cell types and spontaneously rhythmic neurons in which electrical activity pursues a limit-cycle oscillation (*2*).

Except in the boldest simplifications [for example (*3*, *4*)] this class of equations has resisted analytic solution. So with few exceptions its robust or qualitative implications—those that survive the inevitable quantitative adjustments demanded by experimental work—are known only insofar as they are revealed by computer simulation (*5*, *6*), graphical analysis (*7*), and analog devices (*8*).

I report here a robust implication of limit-cycle kinetics in oscillator preparations, such as sensory neurons, spontaneously rhythmic smooth muscle, and the pacemaker regions of the heart. The behavior to be described follows analytically [using the methods of differential topology (*5*, *9*)] from (i) the existence of a limit cycle in the descriptive equations, regardless of the numerical values of measured parameters and of the number of variables encompassed, and (ii) the application of a stimulus which, if sufficiently prolonged, arrests the prior oscillation, regardless of the physical nature of the stimulus. Prolonged hyperpolarization might be an example of such a stimulus. Both (i) and (ii) suffice to account for a newly observed pattern in the way a neural oscillator adjusts the phase of its rhythm after a stimulus impinges on it.

Consider any nerve preparation generating rhythmic action potentials or the smooth subthreshold oscillations revealed by tetrodotoxin in pacemaker membranes (*2*). It will be convenient to take that regular period as our unit of time. Define the instantaneous "phase" as the time elapsed since the most recent voltage maximum (or, in the presence of noise, some best estimate of that time) based on extrapolation of the preceding rhythm. Now let a stimulus impinge on the preparation—for example, an inhibitory postsynaptic potential (IPSP) or a current pulse—following which the preparation soon resumes its previous rhythmic activity, with the same period, but generally with a new phase relative to the extrapolated prior rhythm.

The phenomenon is most readily described in terms of a "resetting curve": a plot of a new phase against an old phase, using data obtained by stimulating at many times in many pacemaker cycles separated by many intervals, as in (*10*, *11*). Just as we extrapolated the prestimulus rhythm forward to estimate the old phase at the stimulus, we now extrapolate the poststimulus rhythm backward to estimate the new phase at the stimulus. In practice (*10–15*), the new phase can be estimated from the timing of only the first poststimulus voltage maximum, if subsequent maxima occur at sufficiently regular intervals [figure 3b in (*12*)]. The shape of this plot depends, of course, on the choice of preparation and the choice of stimulus (such as, a voltage pulse or a burst of inhibitory or excitatory postsynaptic potentials of some duration from some afferent synapse). If, as in the data replotted below from (*10*, *13–16*) and in (*11*, *17*), this curve can be smoothly plotted, then the following features are obtained.

1) The new phase must rise vertically and fall back, or rise or fall through a full cycle, per horizontal cycle of the old phase. This is because the new phase obtained at a given old phase must be the

same in every cycle. Viewed topologically, the new phase and the old phase are periodic coordinates, more properly represented along circles than along Cartesian coordinate axes, so the new phase–old phase plane is really the unrolled surface of a torus (anchor ring, doughnut). Rolled back into that shape, the data curve is seen as a closed ring, which either does or does not thread the hole in the doughnut. These two choices correspond to the two distinct types of resetting data obtained empirically.

2) In the limiting case of small stimuli the new phase rises through one cycle per cycle of the old phase (that is, the new phase never differs much from the old phase). Curves of this type [type 1 (*18*)] were obtained by Sano (*19*) from the rabbit sinus node, by Ayers and Selverston (*10*) from the lobster pyloric network (Fig. 1A), and by Hartline (*11*) from a stretch receptor in *Procambarus*.

3) If the stimulus strength exceeds some threshold, the new phase just rises and falls back, scanning zero cycles per cycle of the old phase. Curves of this type (type 0) were obtained by Perkel and co-workers (*13, 14*) from the thoracic stretch receptor of *Procambarus*, by Pinsker (*15*) from the abdominal ganglion of *Aplysia*, by Walker (*16*) from the chirp reflex of a cricket, and by Taddei-Ferretti (*17*) from *Hydra* (Fig 1, B to D).

4) At the threshold of the stimulus magnitude for transition between types 0 and 1, there must occur an old phase at which the resetting inflicted by the stimulus is not reproducible; that is, there must be an abrupt discontinuity in the data, or the preparation must cease to fire rhythmically at unit intervals. In support of this claim we refer the reader to Guckenheimer (*9*) and note that such a singular stimulus has been demonstrated in three areas of biophysical limit-cycle kinetics which exhibit the foregoing features: in circadian rhythms (*18, 20*), in the yeast cell's oscillating glycolysis (*21*), and in the geotropic oscillation of plant seedlings (*22*).

5) Best (*5*) has used the original Hodgkin-Huxley equations for *Loligo* (*1*) to compute new phase–old phase curves for voltage pulses of various sizes, both hyperpolarizing and depolarizing. Although kinetics in squid axon is nearly discontinuous, he finds features 1 to 4 above, with the membrane current-biased for spontaneously repetitive activity.

These features do not appear in some other kinds of model. For example, new phase–old phase curves in the falling threshold and rising generator potential models of (*2, 11, 13, 14*) exhibit a discontinuous jump at all nonzero IPSP durations, or at all hyperpolarizing currents exceeding some threshold in the physiological range. These are neither type 1 nor type 0. This model seems a reasonable approximation to the nearly discontinuous voltage behavior of some membranes, such as squid axon (*1, 2, 5, 6*), and some resetting curves do appear correspondingly discontinuous [for example, figure 1b in (*10*), figure 2a in (*14*), and figure 5 (1-second pulse) in (*15*)]. But when the near-discontinuity of mechanism is smoothed out over an empirically observable range of phase, as in the sinusoidal generator potentials of heart and smooth muscle (*2*) and the bursting neuron of *Aplysia* (*15*), or by precise computation as in (*5*), then the resetting curve types become observable.

The effect of tonic stimuli on a pacemaker neuron is sometimes described verbally as causing an advance or delay by temporarily accelerating or retarding progress through its electrical cycle. No model of this sort can produce a type 0 resetting curve (*23*).

In preparations exhibiting type 0 resetting (as in Fig. 1, B to D), item 4 above strongly implies the existence of a critical phase at which some briefer or more attenuated stimulus of the same kind must result in unpredictable rephasing. In at least one model (*5*) this corresponds to restoring the membrane to a stable resting potential, thus terminating its spontaneous activity.

The topological distinction between type 1 and type 0 resetting and the existence of a singular stimulus may play roles in the regulation of rhythmical neural activity, as in sensory and proprioceptive neurons, in the heartbeat, and in motor coordination for running, swimming, and flying (*24*).

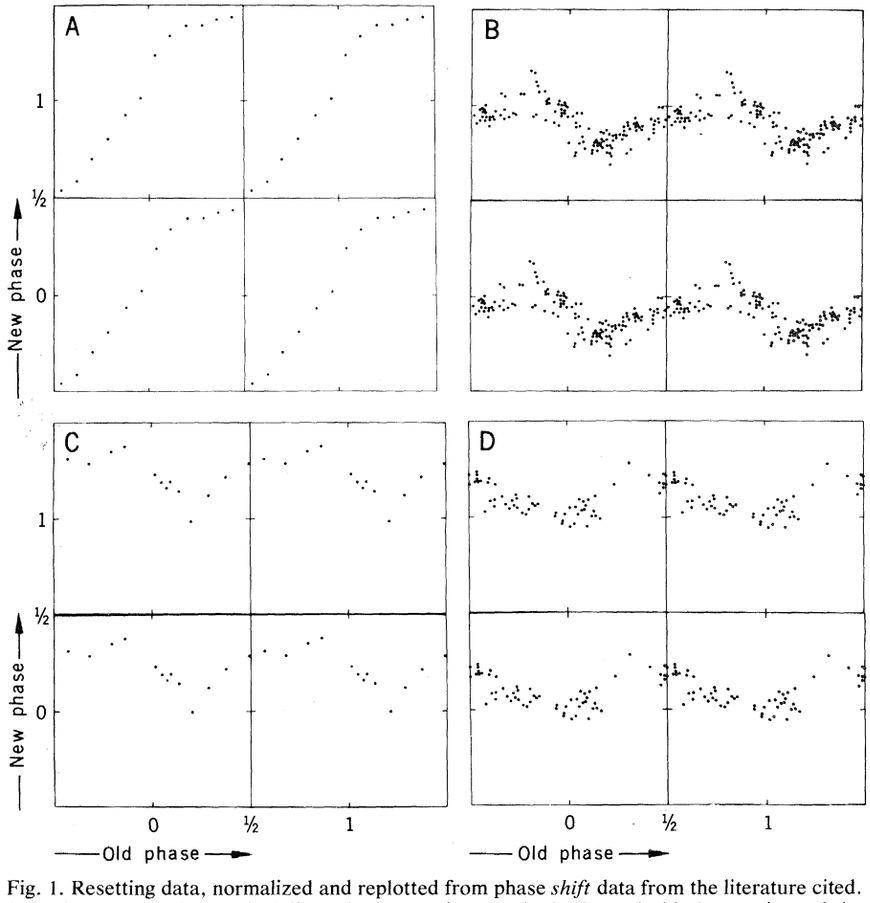

Fig. 1. Resetting data, normalized and replotted from phase *shift* data from the literature cited. In each case the stimulus is delivered at some time on the horizontal old-phase axis, and the reset rhythm's new phase (evaluated at stimulus time as old phase plus the phase advance) locates the data dot vertically. Phase 0 or 1 marks the beginning of the activity burst. (A) Lobster pyloric bursting network reset by synaptic IPSP's; type 1 [figure 1a in (*10*)]. (B) Crayfish thoracic stretch receptor reset by synaptic IPSP's; type 0 [figure 2b in (*14*)]. (C) *Aplysia* bursting neuron, reset by synaptic IPSP's; type 0 [figure 9E in (*15*)]. (D) Cricket stridulation, reset by acoustic detection of a recorded cricket chirp; type 0 [figure 3 in (*16*)]. Each phase axis is duplicated (resulting in fourfold replication of data) to bring out the continuity and symmetry type of the data. Note that all these resetting curves are smooth, even as they pass through the activity burst at old phase 0 or 1.

A. T. WINFREE
Department of Biological Sciences,
Purdue University,
West Lafayette, Indiana 47907

References and Notes

1. A. Hodgkin and A. F. Huxley, *J. Physiol. (London)* **117**, 500 (1952).
2. J. J. B. Jack, D. Noble, R. W. Tsien, *Electric Current Flow in Excitable Cells* (Clarendon, Oxford, 1975).
3. H. P. McKean, *Adv. Math.* **4**, 209 (1970).
4. W. C. Troy, *Proc. R. Soc. Edinburgh Sect. A* **74**, 23 (1975).
5. E. N. Best, thesis, Purdue University (1976).
6. J. Cooley, F. Dodge. H. Cohen, *J. Cell. Comp. Physiol.* **66**, 99 (19 → K. S. Cole, H. A. Antosiewicz, P. Rabinowicz, *J. Soc. Ind. Appl. Math.* **3**, 153 (1955).
7. R. Fitzhugh, *J. Gen. Physiol.* **43**, 867 (1960); *Biophys. J.* **1**, 445 (1961); O. Gurel, *Int. J. Neurosci.* **5**, 281 (1973).
8. L. D. Harmon, *Science* **146**, 1323 (1964).
9. J. Guckenheimer, *J. Math. Biol.* **1**, 259 (1975).
10. J. L. Ayers and A. I. Selverston, *J. Physiol. (Paris)*, in press.
11. D. Hartline, *Brain Res.* **110**, 245 (1976).
12. H. M. Pinsker and E. R. Kandel, *ibid.*, **125**, 51 (1977).
13. G. P. Moore, J. P. Segundo, D. H. Perkel, in *Proceedings of the San Diego Symposium for Biomedical Engineering*. A. Paull, Ed. (San Diego Symposium for Biomedical Engineering, La Jolla, Calif., 1963), pp. 184–193.
14. D. H. Perkel, J. H. Schulman, T. H. Bullock, G. P. Moore, J. P. Segundo, *Science* **145**, 61 (1964).
15. H. M. Pinsker, *J. Neurophysiol.*, **40**, 527 (1977).
16. T. J. Walker, *Science* **166**, 892 (1969).
17. C. Taddei-Ferretti and L. Cordelle, *J. Exp. Biol.*, **65**, 737 (1976).
18. A. T. Winfree, in *Biological and Biochemical Oscillators*, B. Chance, E. K. Pye, B. Hess, Eds. (Academic Press, New York, 1973), pp. 461–501.
19. T. Sano, unpublished observations.
20. W. Englemann, H. G. Karlsson, A. Johnsson, *Int. J. Chronobiol.* **1**, 147 (1973); D. S. Saunders, *J. Comp. Physiol.* **110**, 111 (1976).
21. A. T. Winfree, *Arch. Biochem. Biophys.* **149**, 388 (1972); L. Greller, thesis, University of Pennsylvania (1977).
22. A. Johnsson and D. Israelsson, *Physiol. Plant.* **22**, 1226 (1969).
23. A. T. Winfree, *J. Interdiscip. Cycle Res.* **8**, 1, (1977).
24. P. S. G. Stein, *Am. Zool.* **14**, 1003 (1974).

25. I thank the National Science Foundation for grant BMS 73 0688 1 and the National Institutes of Health for a research career development award, J. Ayers for use of data prior to publication, T. Sano for use of unpublished data, and H. Pinsker for guidance to current literature.

23 March 1977

Water-to-Air Transfer of Virus

Abstract. *Bubbles rising through suspensions of the bacteriophages T2 and T4 and of* Escherichia coli *adsorb and eject these particles in droplets that are formed when the bubbles burst. The concentration of the viruses in ejected droplets, determined from electron microscopy, exceeded the suspension concentration by 50 times. Similar results were obtained for* Escherichia coli. *The viability of some of the adsorbed particles was established by biological counts.*

This study concerns the possibility that bubbles adsorb viruses and propel them into the atmosphere when the bubble bursts. Bubbles bursting at a liquid surface eject a tiny jet of fluid into the air. The jet breaks up into a series of tiny drops with the diameter of the uppermost drop one tenth that of the bursting bubble (*1*) and with most of the lower drops having larger diameters. Such jet drops contain much of the material adsorbed to the bubble (*1*) as well as some of the material adsorbed to the surface of the liquid (*2*).

Transport into the atmosphere of red-tide toxins (*3*), organic matter (*4*), and bacteria (*1*) has previously been related to aerosol formation. Gruft *et al.* (*5*) postulated that aerosol of marine origin is a vector of *Mycobacterium intracellulare* (Battey) infection. Whether pathogenic viruses are similarly airborne is clearly of public health concern.

In the present study, the coliphages T2 and T4 were chosen as harmless indicator viruses which, after aerosol ejection, could be assayed biologically and morphologically. If these viruses, with their complex structure and sensitivity to drying and ultraviolet radiation, remained viable and became concentrated during aerosol formation, then it could be assumed that the simpler, less fragile viruses are similarly dispersed.

The jet droplets used in this study were formed by admitting air bubbles (0.03 cm in diameters) under pressure (1 to 2 kg/cm^2) (*6*) into the bottom of a liquid column (17 cm in depth) containing *Escherichia coli* and the bacteriophages suspended in buffer. The phage concentration was adjusted to 5×10^8 per milliliter and the bacteria to a concentration of 5×10^6 per milliliter.

Depending on the experiment, different suspending fluids were used in the column. Jet droplets containing phage were seen in the electron microscope when the phages were suspended in tris buffer (0.1*M*, *p*H 7.6, with 3 percent NaCl). The phage lysate and washed bacteria were added to distilled water. Lysate facilitated adhesion of jet droplets to the carbon film of the electron microscope grid, and upon drying left a distinct circular contour which we used for diameter measurement.

The T2 and T4 bacterial viruses were prepared in high titers from lysates of their host cell B/1,5 (a strain of *E. coli*) grown in synthetic medium (*7*) with heavy aeration. In some experiments the phages were centrifuged away from the lysate and resuspended in buffer before they were added to the column. *Escherichia coli* B/4, a strain that is resistant to T2 and T4, was grown overnight in 1 percent tryptone broth with aeration at 37°C to the stationary phase. The cells were centrifuged and the pellet was suspended in the same buffer as that used in the bubble chamber.

To collect jet droplets for electron microscopy, grids bearing carbon films were held inverted for 30 to 45 seconds about 1 cm above the surface where the bubbles were bursting. In this configuration of emitting bubbles and collecting surface we collected the uppermost two or three droplets of the jet (*8*). The collected droplets were dried in air for 1 minute to minimize subsequent loss of material, stained in saturated uranyl acetate for 2 minutes, rinsed in distilled water, drained, and dried.

The specimens were photographed at two magnifications (×3000 and ×10,000) by means of a Jeolco 100B electron microscope at 60 kv. Enlarged prints at the lower magnification were used for diameter measurements of the dried droplets and for counting the number of viruses and bacteria in measured areas. The smallest area used in the counts was a quadrant. Only particles showing both a head and an extended tail were counted as virus.

The fields photographed at the higher magnification were randomly selected and provided morphological evidence of intact virus in the droplets.

Viability assays were obtained by holding moist petri dishes containing tryptone agar above the surface of the bubble column for 10 to 40 seconds. Soft agar (0.7 percent) was immediately added to the surface of the dish and spread by vigorous shaking. In the case of the phage assays the soft agar contained the sensitive cell, B/1, 5. The dishes were incubated overnight at 37°C.

Electron microscopy showed that both phages and bacteria were transferred from bulk fluid into air by jet droplets. The mean volume calculated from 18 droplets was $2 \times 10^{-8} \pm 1 \times 10^{-8}$ ml (± standard deviation) with a range of 4×10^{-8} to 7×10^{-9} ml. Thus the range of diameters of drops ejected from bubbles that were 300 μm in diameter was 24 to 42 μm, the mean being 34 μm. These data corroborate Blanchard's (*1*) rule of thumb that the diameter of the top drop of the jet set is one-tenth the diameter of the bubble. The range of drop sizes results from collecting the uppermost three drops. The second and third drops of the set are smaller and larger, respectively, than the top drop.

The number of phages per droplet was determined from the electron micrograph by counting the number of particles having both a head and a tail per unit area of droplet. Bacteria were easily identified by shape and size. Eighteen separate droplets captured from a col-